

Ground-based SAR interferometry as a supporting tool in natural and man-made disasters

Andrea Di Pasquale¹, Marco Corsetti², Pietro Guccione³, Andrea Lugli⁴, Marco Nicoletti¹, Giovanni Nico⁵ and Mariantonietta Zonno³

¹*DIAN srl, Matera, Italy; a.dipasquale@dianalysis.eu*

²*Università di Roma "La Sapienza", DICEA, Rome, Italy; marco.corsetti@uniroma1.it*

³*Politecnico di Bari, DEI, Bari, Italy; p.guccione@poliba.it*

⁴*Università di Bologna, DICAM, Bologna, Italy; andrea.lugli8@unibo.it*

⁵*CNR-IAC, Bari, Italy; g.nico@ba.iac.cnr.it*

Abstract. In this work we present some applications of Ground-Based Synthetic Aperture Radar (GBSAR) interferometry to the monitoring of dams, bridges and landslides. A SAR system is a coherent active microwave device able to provide 2D refractivity images of a given area with high spatial resolution, independently of weather conditions and day-night cycle. SAR interferometry is the most notable application of SAR technology. This technique relies on the processing of a time series of coherent SAR images. It gives a powerful tool to produce maps of deformations occurring in infrastructures (dams, buildings, bridges) or terrain. In the last few years the research activity of several remote sensing groups has dealt with the development of GBSAR systems. GBSAR sensors represent a cost-effective solution for the continuous monitoring of small scale deformation phenomena if compared to space and air-borne systems. These systems basically consist of a CW radar mounted on a sliding support and synthesizing in time an aperture longer than the physical dimension of their real antennas. The main advantage of GBSAR displacement measurements, provided with a sub-millimetre accuracy, is that they provide the spatial pattern of the deformation phenomenon and not only measurements in a few selected points as in the case of traditional geotechnical instruments. Some examples of application of GBSAR technology are described. The GBSAR results are compared to measurements obtained by traditional instruments.

Keywords. Synthetic Aperture Radar (SAR), Ground-based SAR (GBSAR), SAR Interferometry (InSAR). Supporting Disaster Management, Natural and man-made disasters.

1. Introduction

In the last decade, Ground-Based Synthetic Aperture Radar systems have gained an increasing interest in different applications ranging from terrain mapping and deformation measurements, to structural analysis of man-made constructions [1]-[4]. A Synthetic Aperture Radar (SAR) is an active microwave sensor used to produce 2D microwave images of the observed scene. The main advantage of microwave images is their capability to observe a scene without the need of solar illumination and in any weather condition. For these reason this kind of sensor has been used in space-borne missions to observe the earth surface. In the last few year, ground-based SAR systems have been developed to solve the problem of continuous monitoring of small scenes, such as dams, landslides, buildings, bridges, or to extract information on terrain morphology. The Ground-Based Synthetic Aperture Radar (GB-SAR) interferometry is a relatively new technique that, in the last ten years, has gained an increasing interest for deformation measurements due to the continuous monitoring capabilities of medium-scale sites. A number of experimental results demonstrated the GB-SAR effectiveness for remote monitoring of terrain slopes and as an early warning system to assess the risk of rapid landslides [5]. This non-destructive radar technique can provide displacements measurements of structures and natural scenes with a sub-millimetre accuracy. A GBSAR system is

installed at a distance from the observed object ranging from less than one hundred metres up to a four kilometres. The interferometric processing of two coherent SAR images results in a map of displacements occurred between the acquisitions of the two SAR images. Radar measurements give the projection along the radar line-of-sight of the 3D displacement vector. The main advantage of GBSAR interferometry with respect to many traditional techniques is its capability to provide 2D information on the displacement field rather than measurements of displacements in only a few points. In this paper we describe the technique, providing details on how SAR images are properly focused and used to generate displacement maps. GB-SAR systems provide some advantages with respect to space and air-borne SAR sensors such as higher image resolution and shorter revisiting time. A single image is acquired in few minutes, while the working range distance to the study area ranges from about less than 100 m up to about 4000 m.

Furthermore, the capability of GB-SAR interferometers to measure deformations with a sub-millimeter accuracy together with their flexibility makes them a useful tool for monitoring landslides and other geological phenomena in emergency cases [5].

The structure of the paper is as follows. Section 2 briefly review the working principles of GBSAR systems and of SAR interferometry. Emphasis is put on the accurate and efficient focusing approaches of radar data depending on the observation configuration. An experiment to assess the accuracy of displacement measurements provided by GBSAR interferometry is described in section 3. Two examples of application of this technique to the monitoring of displacements of dam and a landslide area are presented in section 4. Finally a few conclusions are drawn in section 5.

2. Methods

A ground-based SAR system is a stepped-frequency radar. A couple of TX/RX antennas are mounted on a computer-controlled positioner that synthesizes a linear aperture along the so called azimuth direction. A microwave source illuminates the observed scene at different discrete frequencies within the frequency band 16.70–16.78 GHz. The length of the synthetic aperture is 2.0 m. The sampling rates in frequency and space are set in order to satisfy the Nyquist criterion. The processing of ground-based, space and airborne SAR data relies on the same physical principles, as the focusing step ideally requires a two-dimensional space-variant correlation of the received echoes with the point scatterer response of the SAR system. However, it is worth noting that a GB-SAR system is characterized by a sub-optimal synthetic aperture, being such a sub-optimality function of the antenna footprint in the azimuth direction. A SAR system is optimal when the synthetic aperture is equal to the antenna footprint. This does not constitute a problem in space and air-borne systems since they continuously acquire radar echoes along the orbit. While, in the case of GB-SAR systems, the synthetic aperture is the rail length which is typically 2-4 meters. An exact focusing method is that of the Frequency-Domain Back-Propagation algorithm (FDBA). This approach is supposed to be applied to a stepped-frequency continuous-wave (SF-CW) or a Multiple-Input Multiple-Output (MIMO) radar and consists in the coherent sum of the stepped frequency contributions at the different radar positions along the aperture, corrected for their phase delay. The computational load associated to this method is $O(M N M' N')$ where (M, N) are the dimensions of the raw data matrix and (M', N') that of the focused image. As for the spaceborne case, a close-to exact focusing can be achieved by the wavenumber-domain algorithm. Such approach, in case of sub-optimal synthetic apertures, can be highly inefficient since a zero padding in azimuth of thousand of samples would result in an unnecessary oversampling of the focused data at the step of the antenna movement along the rail. However such an inefficiency decreases for near fields making this algorithm more convenient for medium to little distances. A further simple and straight approach, known as Time-Domain focusing Algorithm, grounds on the fact that the radar echoes after range compression can be written as a convolution between the reflectivity map of the scene and the system impulse re-

sponse. At far ranges, this convolution is interpreted as a product in the frequency domain of the range compressed data along the azimuth direction and the system transfer function. Thus, focusing is a simple multiplication and Fourier transform. This approach is the less precise but also the fastest and hence it is commonly adopted for far-field focusing. Time Domain Algorithm can be considered well suited for the far range case (let's say $> 300\text{m}$), as the migration effects introduced are minimal (less than $1/2$ of sampling step) and the phase error moderate (below 1rad at center, less at scene borders). On the contrary, A Wavenumber Domain Algorithm is the correct choice to process images acquired at near range, less than 50m . If the purpose of acquisition is the analysis of vibrations or the long-term monitoring of subsidence, low image distortion is required and TDA is no longer suited, as implications on interferogram quality are straight [6]. The spatial resolution in range is 0.75 m while that in azimuth depends on the distance between the radar and the observed scene as described by the following relationship

$$\Delta x = \frac{\lambda R}{2L}, \quad (1)$$

where Δx is the azimuth resolution, λ the radar wavelength, R the range distance and L the synthetic aperture. In interferometric applications a GBSAR system acquires a time series of SAR images of the scene with a minimum sampling period of five minutes. Each SAR image is a complex image bearing both amplitude and phase information. Amplitude is related to the scattering properties of the scene while the phase depends on its geometry and displacements. For each pair of SAR images acquired in an interferometric configuration, an interferometric phase image is computed as follows

$$\Delta\varphi = \arctan\{S_1 \cdot \text{conj}(S_2)\}, \quad (2)$$

where $S_1 = |S_1| \exp(i\varphi_1)$ and $S_2 = |S_2| \exp(i\varphi_2)$ are the two coherence SAR images acquired at time t_1 and t_2 . A displacement D at a point P in the scene is related to the interferometric phase by the relationship

$$D = \frac{\lambda}{4\pi} \Delta\varphi \quad (3)$$

where λ is the radar wavelength that for the radar used in this application is $\lambda = 18\text{ mm}$. The most important issue when performing interferometric radar measurements is that of interferometric coherence. This depends on both the properties of the observed scene and the acquisition configuration. For example an area covered by a huge vegetation gives rise to coherence losses due to random movements of leaves and branches also in mild wind conditions and, as a consequence, displacement measurements are noisier. In the case of both earth and concrete dams, this source of decorrelation is not present so providing an ideal application field. Besides decorrelation effects induced by the scene properties, the capability to re-install the GBSAR system at the same position with an accuracy of a few millimetres can also affect interferometric coherence even in the case of dam monitoring. A way to solve this problem consists in constructing a temporary fixed structure in front of the dam, easily removable if needed, so as to accurately re-positioning the GBSAR rail. **Errore. L'origine riferimento non è stata trovata.** shows an example of temporary fixed structure used to re-positioning a GBSAR system avoiding coherence losses. As can be observed in equation (3) the accuracy of displacement measurements depends only on the accuracy of phase measurements. Usually phase measurements in radar systems have an accuracy about 30 degrees for mildly decorrelated scene. This corresponds to an accuracy of $\lambda/24$ in displacement measurements. Decorrelating phenomena reduce the accuracy of phase measurements so affecting also the accuracy of displacement measurements. At the radar frequency used in this campaign, the measurement accuracy is a fraction of millimetre. It is worth noting that the accuracy of the radar position coordinates does not affect the accuracy of displacement measurements. In fact, the knowledge of radar position coordinates is needed only for the rendering of displacement measurements on the dam surface and does not enter the interferometric processing of radar data.

3. Accuracy and precision of GBSAR displacement measurements

In this section we describe an experiment which has been carried out to assess both the precision and accuracy of GBSAR displacement measurements. A corner reflector mounted on a micrometric screw was used (see Figure 1). The scheme of the experimental setup is reported in Figure 2. Fourteen SAR images were acquired on July 27th, from 06:47 pm to 07:52 pm. Table 1 summarizes the acquisition times of the SAR images as well as the corresponding positions of the micrometric screw. A set of thirteen interferograms was generated by processing the each SAR image with the subsequent one.



Figure 1. Corner reflector used to assess the precision and accuracy of GBSAR displacement measurements.

For example, Figure 3 displays the interferogram obtained by processing the SAR images acquired at 06:52 pm and 06:57 pm. During this 5-minute temporal baseline the micrometric screw was displaced of 5 mm in the down-stream direction. This caused a decrease of the range distance between the GBSAR and the corner reflector. As a result a small patch of negative phase pixels appeared in the interferogram located at a range distance of about $R=70$ m and an angular position of about $\phi = 6$ degrees (see also the detail reported in Figure 4.).

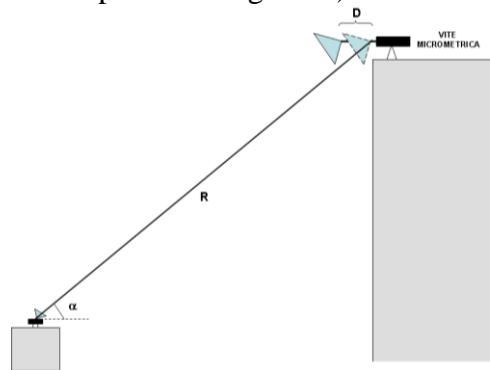


Figure 2. Scheme of the experimental setup.

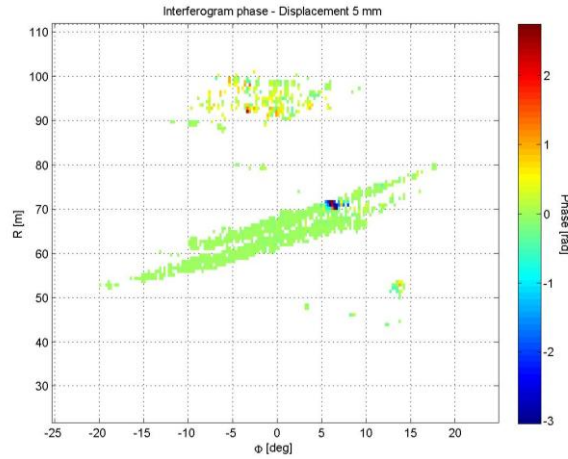


Figure 3. GBSAR Interferogram of the dam obtained by processing SAR images acquired on July, 27th at 06:52 and 06:57 m. The blue spot corresponds to the 5 mm displacement of corner reflector occurred between the acquisition of SAR images.

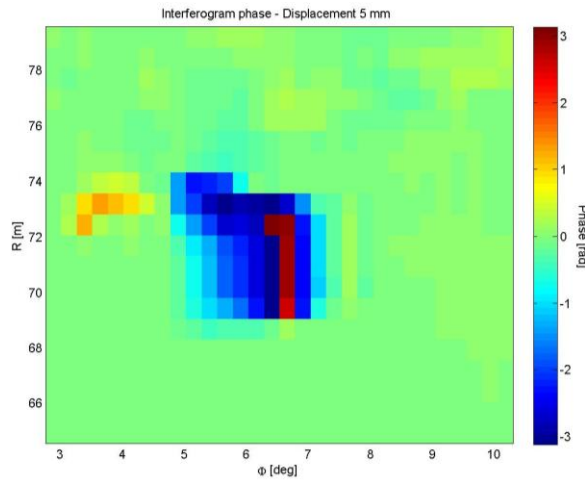


Figure 4. Detail of GBSAR interferogram displayed in Figure 3. around the location of corner reflector.

The displacement of corner reflector in the Line-of-Sight direction was obtained using the relationship (3). Finally, the true displacement along the down-stream direction was obtained correcting for the geometrical configuration as

$$D_{DS} = \frac{\lambda}{4\pi} \frac{1}{\cos \alpha} \Delta\varphi \quad (4)$$

where α is the antenna elevation angle (see Figure 2). The final result is estimated in Figure 5, which reports the position of corner reflector along the time needed to acquire the fourteen SAR images. The estimated position of corner reflector is represented as a green star. The comparison with the true positions of corner reflector reported in the third column of Table 1 shows that the GBSAR interferometry technique manage to estimate the position of corner reflector with a sub-millimeter accuracy and its displacements with both a sub-millimeter accuracy and precision.

Table 1. Positions of micrometric screw at the acquisition times of SAR images. All images were acquired on July, 27th, 2012. The corner reflector is moved by the micrometric screw.

N. of SAR image	Acquisition Time	Position of micrometric screw [mm]	N. of SAR image	Acquisition Time	Position of micrometric screw [mm]
1	18.47.42	10	8	19.22.28	2
2	18.52.40	10	9	19.27.26	2
3	18.57.38	5	10	19.32.23	2
4	19.02.36	5	11	19.37.21	1
5	19.07.35	5	12	19.42.19	1
6	19.12.33	5	13	19.47.16	1
7	19.17.30	2	14	19.52.15	1

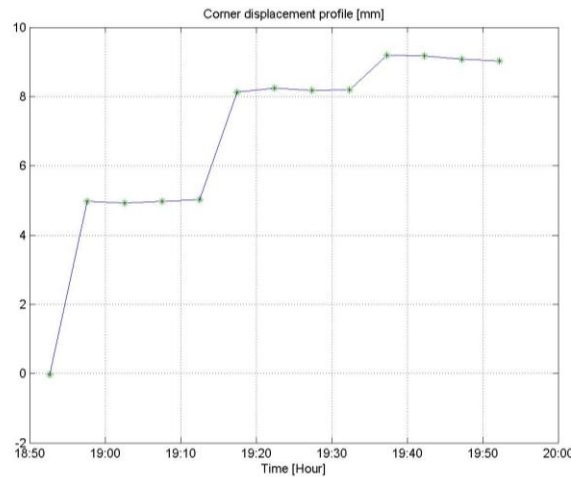


Figure 5. Displacements of corner reflector measured by GBSAR interferometry vs acquisition times of SAR images.

4. Results

In this section three examples of application of GBSAR interferometry will be described. The first example concerns the monitoring of displacements of a dam surface due to changes in water level and temperature. The second example describes the application of GBSAR interferometry to measurement of terrain displacements induced by a mass movement.

Figure 6 displays the map of dam deformations measured by the GBSAR system during a 12-hour continuous monitoring campaign. The map is rendered on the mesh of the dam surface. Positive displacements mean that the dam distance from the radar increased, i.e. a up-stream displacement occurred. A maximum displacement of about 3 mm in the up-stream direction was observed at the centre-top of dam. This maximum displacement is not located at the crown where a mark of the permanent topographic monitoring system is installed, but a few meters below.

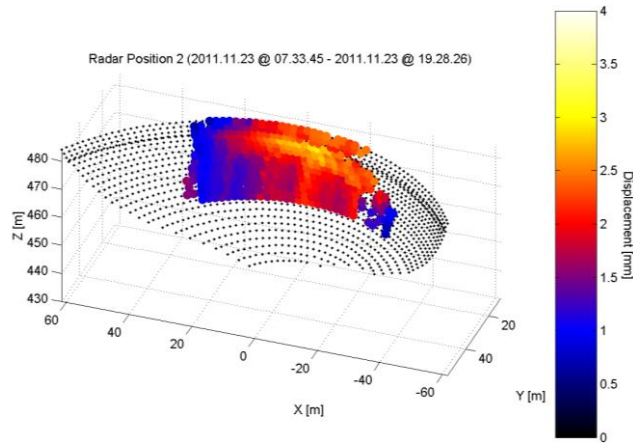


Figure 6. Map of displacements rendered on the dam surface.

To facilitate the inspection of displacement maps, the time series of GBSAR measurements were extracted at eight points selected along the dam centerline and at the top of the dam (see Table 1). The time series of dam displacements measured by the GBSAR system at points {P1, P2, ... P8} are reported in Figure 7. The time series are characterized by a similar periodic behavior with a maximum amplitude depending on the point location. Displacement measurements at point P5 and P6 are noisier than those at the remaining points due to the fact that points P5 and P6 are located at the border of the radar main beam and as a consequence have a lower signal-to-noise ratio and a noisier interferometric phase. As a validation of GBSAR measurements, displacements measured by the radar system at points P1, P5 and P6 were compared to topographic measurement of three marks located at the top of the dam (see Figure 8). It is worth noting that when comparing radar and topographic measurements we should be aware that these measurements have different properties. The traditional topographic system provide the displacement of a mark located at the crown of the dam. Instead, the GBSAR system provides the mean displacement of a small area of less than 1m X 1m on the dam surface.

Table 2. Coordinates of points P1, P2, P3, P4, P5, P6, P7 and P8 located on the dam surface.

Point	X [m]	Y [m]	Z [m]
P1	0	20.6000	484
P2	0	22.3000	480
P3	-14.1200	23.7500	480
P4	15.6600	24.0800	480
P5	-29.5100	28.8500	480
P6	30.5300	29.3400	480
P7	0	16.6600	470
P8	0	10.4200	450

Results presented in Figure 7 are useful to describe the capability of the GBSAR system to provide accurate displacement measurements of the dam surface during a continuous monitoring campaign. This kind of data acquisition strategy is the typical one of traditional techniques used to monitor dams. A different monitoring paradigm consisting in re-installing the GBSAR system after a period varying from a three to six months has been also adopted.

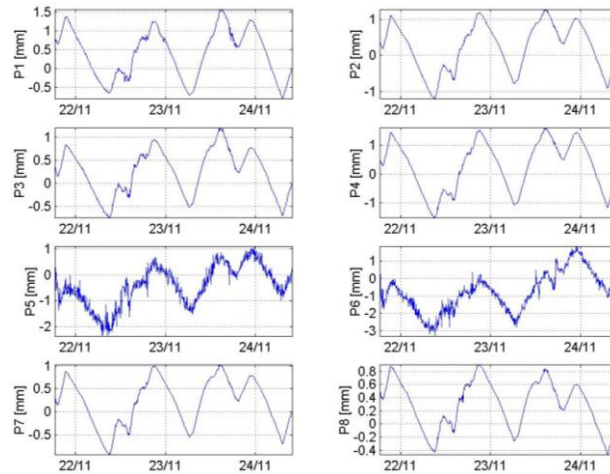


Figure 7. From the top-left to bottom-right, the time series of dam displacements at the eight points of Table , measured by the GBSAR system by November, 21st 2011, 4 a.m to November, 9th 2011.

Figure 9 displays the map of dam displacements measured by the GBSAR installed at position 1. The map was obtained by processing the SAR images acquired with a temporal baseline of 106 days. The two images were acquired during the first and second campaign, respectively, after having re-positioned the GBSAR system. As a first consideration we observe that the map in Figure 9 is in radar coordinates (range and angular direction) and was not geolocated on the dam surface. The reason for this is to describe a procedure to read maps displayed in radar coordinates and to facilitate the recognition of dam sectors. The procedure consists in projecting the element of the dam mesh into radar coordinates. Figure 9 shows as open black circles the mesh points having an altitude of $z=484$ m and $z=455$ m, respectively. Furthermore, the mesh point lying along the centerline are also plotted as a dashed green line. The map in Figure 9 shows at the top ($z = 484$ m) of the dam a up-stream displacement up to 3.5 mm, in correspondence of the centerline, and a down-stream displacement up to 2 mm at $z = 455$ m. The comparison with topographic measurement of mark 3 for a temporal interval around the acquisition times of the two SAR images, see Figure 10, shows that the topographic system measured a up-stream displacement of about 3 mm, in agreement with the GBSAR measurement at the top of the dam. However, the available topographic measurements does not allow the validation of the GBSAR measurement at $z = 455$ m.

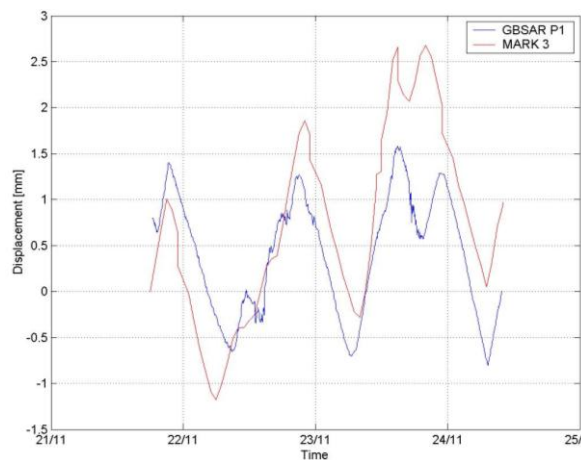


Figure 8. Displacements measured, respectively, by the GBSAR system and the topographic system at P1 and mark 3. Measurements refer to the time interval between November, 21st 2011, 4 a.m and November, 9th 2011.

A simulation of the elastic behavior of the dam between November 20th at 10:56 a.m. and March 5th at 10:58 a.m. was run to validate the GBSAR map of Figure 9. Both changes in the water level and temperatures was taken into consideration. The result of simulation, shown in Figure 11, seems to confirm the differential displacement of the dam, a up-stream movement at the top and a down-stream displacement at a lower height. This comparison also shed light on the usefulness of the 2D displacement information provided by the GBSAR. It is worth noting that the choice of very long temporal baselines could require a more sophisticated processing of GBSAR phase data due to the phase wrapping phenomenon [4]. To conclude this section, we emphasize that the whole acquisition, storage and processing of GBSAR data and the presentation of displacement information to final user can also be performed in a distributed computational environment with machines dedicated to the storage of data directly controlled by the final users that if needed can provide access to the data for more advanced processing or use GBSAR 2D displacement maps for numerical studies [5].

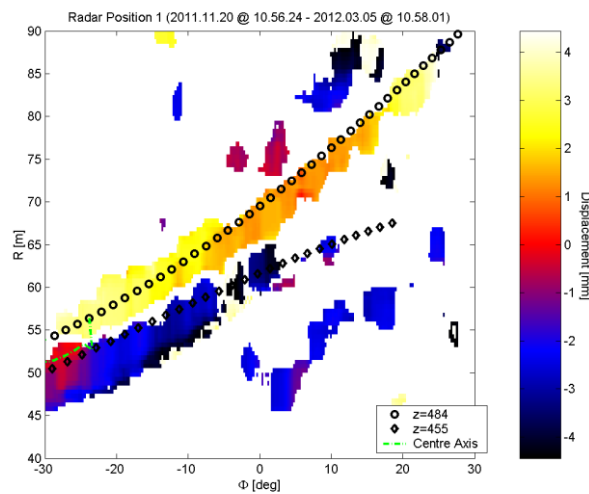


Figure 9. Displacement map referred to the time interval between November 20th at 10:56 a.m. and March 5th at 10:58 a.m.

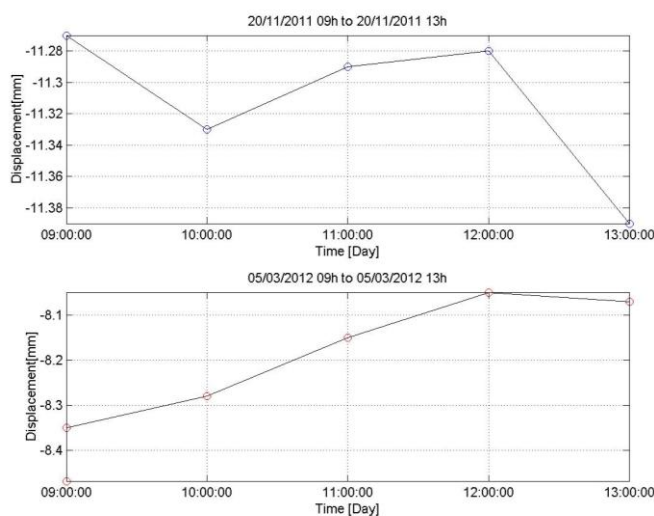


Figure 10. Position of mark 3 in around the acquisition times of the two SAR images of Figure 9. The displacement value is obtained by subtracting the mark position in November from that in march.

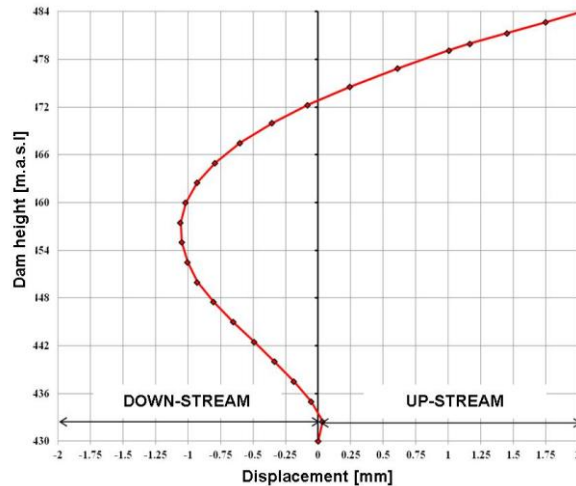


Figure 11. Dam displacement at the centerline simulated by the SAP 2000. Displacements are referred to the time interval between the first and the second campaign.

As a further application of GBSAR interferometry we describe an example of 24-hour monitoring campaign of a landslide area in the Municipality of Aliano, Basilicata Region, southern Italy. The landslide directly affect the stability of the bridge accessing the village as shown in Figure 12. The GBSAR system has been installed at a distance of about 900 m from the bridge in order to image the area. Figure 13 displays the amplitude SAR image of the landslide area. It can be easily recognized the red linear structures in the middle of the image corresponding to the two portion of the bridge observed the radar position. The V-shaped area at the bottom the linear structures represents the landslide area with the red spot located at the azimuth angle $\psi = -5^\circ$ and range distance $R = 750$ m corresponds the outcrop shown in figure 14. The orange-to-yellow area beyond the linear structures represents the radar signal scattered by the hill just after the bridge. The displacement map provided by GBSAR interferometry in a 24-hour measurement campaign is displayed in Figure 14. The map has been obtained by processing the two SAR images acquired at the beginning and the end of the monitoring campaign. White pixels represents portions of the map which have been masked out due to the low signal-to-noise ratio of radar signal. To better follow the temporal evolution of terrain displacements of the area the outcrop location, all SAR images were interferometrically processed, taking the SAR image acquired at the beginning of the campaign as master image and the SAR images acquired at later times as slave image. On the resulting displacement maps, a squared area of 10x10 pixels centered around the outcrop location was statistically analyzed to estimate both the mean displacement value and its standard deviation. The resulting profile is shown in Figure 15 where it can be observed that a small acceleration has been measured starting from the 5 a.m., possibly triggered by the night-time rain.

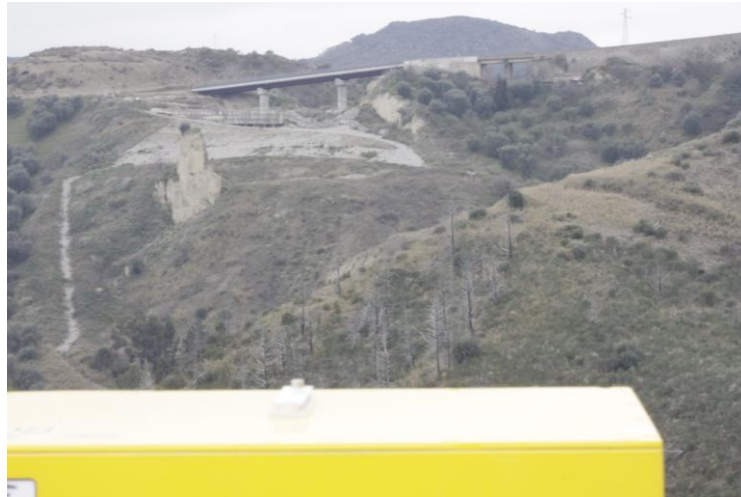


Figure 12. View of the landslide area.

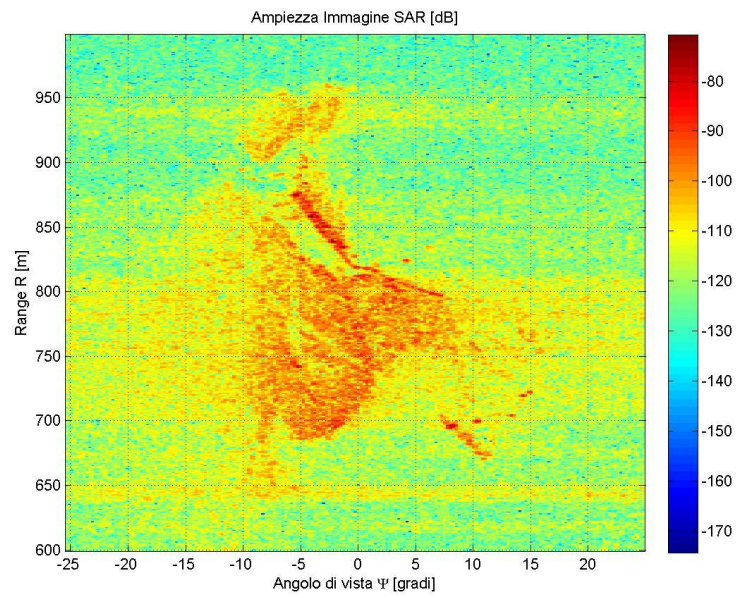


Figure 13. SAR image amplitude of the landslide area.

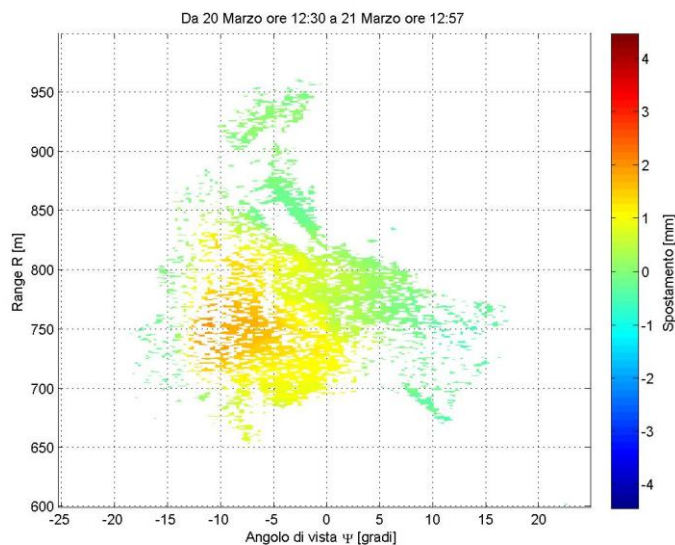


Figure 14. Displacement map of the landslide area measured in a 24-hour campaign.

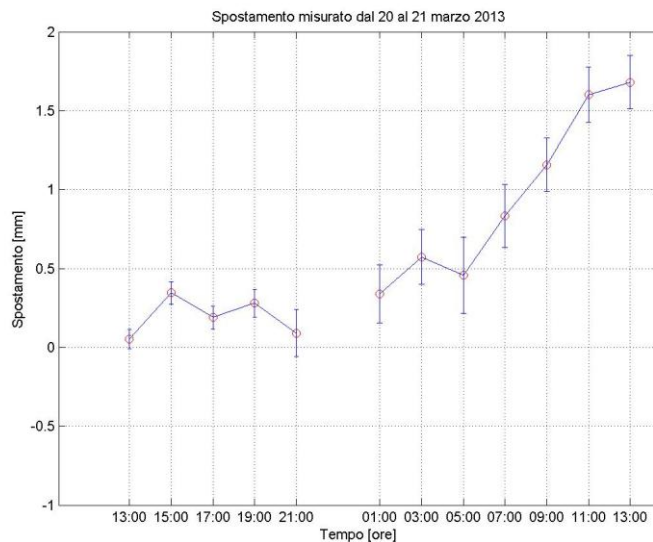


Figure 15. Temporal profile of terrain displacement around the outcrop location.

5. Conclusions

In this work we described the basic principles of GBSAR interferometry and presented two applications of this technique for the real-time monitoring of displacements in dams and landslide areas. It was emphasized how the raw-data acquired by the GBSAR system should be properly processed, depending on the kind of observation configuration, near or far range, in order to both save computational time and provide correctly focused SAR images. The results presented in this paper suggest that this technique can provide a useful tool for the mitigation of natural and infrastructural hazards and for civil protection operation during emergencies.

References

- [1] Leva, D., Nico, G., Tarchi, D., Fortuny-Guasch, J., Siber, A.J., *Temporal analysis of a landslide by means of a ground-based SAR interferometer*. IEEE Transactions on Geoscience and Remote Sensing, vol. 41(4), 745-752, 2003.
- [2] Pieraccini, M., Luzi, G., Mecatti, D., Fratini, M., Noferini, L., Carissimi, L., Franchioni, G., Atzeni, C., *Remote sensing of building structural displacements using a microwave intererometer with imaging capability*, NDT & E International, vol. 37, 545 – 550, 2004.
- [3] Nico, G., Leva, D., Fortuny-Guasch, J., Antonello, G., Tarchi, D., *Generation of digital terrain models with a ground-based SAR system*, IEEE Transactions on Geoscience and Remote Sensing, vol. 43(1), 45 – 49, 2005.
- [4] Pipia, L., Fabregas, X., Aguasca, A., Lopez-Martinez, C., Duque, S., Mallorquí, J.J., Marturía, J., *Polarimetric differential SAR interefrometry: first ersults with ground-based measurements*, IEEE Geoscience and Remote Sensing Letters, vol. 6(1), pp. 167 – 171, 2009.
- [5] Antonello, G., Casagli, N., Farina, P., Leva, D., Nico, G., Sieber, A.J., Tarchi, D., *Ground-based SAR interferometry for monitoring mass movements*, Landslides, vol. 1(1), pp. 21 – 28, 2004.
- [6] Guccione, P., Zonno, M., Mascolo, L., Nico, G., 2013. *Focusing algorithms analysis for ground-based SAR images*. IGARSS Proceedings 2013 (in press)
- [7] Nico, G., Corsetti, M., Di Pasquale, A., Donnarumma, D., Dotti, L., Fiorentino, L., Nicoletti, M., 2013. *On the monitoring of dams by means of ground-based radar interferometry (GB-SAR)*. 9th ICOLD European Club Symposium Proceedings 2013 (in press)

